

Supplementary Online Materials

Ethics statement

This study was conducted in accordance with the Helsinki Declaration, with written informed consent obtained from the patients' families. Approval for this study was obtained from the French Ethics Committee "Comité de Protection des Personnes" (CPP), The French National Agency for Medicine and Health Product Safety (ANSM) and the *Institut National de la Santé et de la Recherche Médicale* (INSERM) in France, and the Rockefeller University Institutional Review Board (IRB), New York, USA.

Case Reports

Kindred A: P1 was born in 2008 to first-cousin consanguineous parents from Turkey (Fig. 1A, III.2). She was vaccinated with BCG at the age of three months and presented left axillary lymphadenitis (5 cm x 5 cm) at 17 months of age. A tuberculin skin test was strongly positive (PPD = 20x20 mm). Initial hemoglobin concentration was 11.8 g/dl, WBC was 13,000/mm³, absolute neutrophil count was 7,000/mm³, and absolute lymphocyte count was 4,700/mm³. Tests for HIV antibody were negative. Serum immunoglobulin levels were normal. Peripheral blood lymphocyte subsets and *in vitro* T-

cell functions were normal. Neutrophil function was normal in terms of respiratory burst, tested in the DHR assay (upon PMA activation). CD212 (IL-12R β 1) expression was normal (CD212: 93% of leukocytes). Chest X-ray findings were normal. Pathology examinations of the lymph node capsule biopsy specimen revealed caseating granulomatous inflammation. Ziehl-Neelsen staining for acid-fast bacilli (AFB) detected such bacilli within histiocytes. *M. tuberculosis* infection could not be confirmed by diagnostic PCR and the *Mycobacterium bovis*-BCG vaccine was suspected. Ziehl-Neelsen staining for AFB was negative for a gastric aspirate sample. The patient was diagnosed with BCG-osis and treated with isoniazid, rifampin, ethambutol and clarithromycin. After two months, ethambutol and clarithromycin treatments were stopped, and isoniazid and rifampin were continued for six months. The patient made a full recovery and has never had *Salmonella* or *Candida* infections.

P2 was born, in 1989, to first-cousin consanguineous parents (Fig. 1A, II.3). P2 had pulmonary tuberculosis at the age of five years, for which he received anti-TB treatment (details not available) and recovered. He has never had *Salmonella* or fungal infections. His family history contains no other remarkable elements and P2 is healthy without treatment.

P3 was born in 1979 and is asymptomatic. P2 and P3 are the uncles of P1.

Kindred B: P4 was born in 1994, to consanguineous parents from Iran (Fig. 1B, II.1). P4 was vaccinated with BCG in early infancy and developed BCG-adenitis with pus discharge, which persisted for one year and then spontaneously resolved. She is now well, with no treatment. Her younger brother, P5, was born in 2006 (Fig. 1B, II.5). He was also vaccinated with BCG in early infancy, after which he developed axillary lymphadenopathy

that did not resolve. At the age of five years, he was admitted to hospital for hepatosplenomegaly and mediastinal lymphadenopathy. He was treated with an antimycobacterial drug regimen, including isoniazid, rifampicin, ethambutol, ofloxacin, clarithromycin, cycloserine, and dapsone, for 1.5 years. He was also treated with exogenous IFN- γ therapy. PPD testing at the age of seven years was negative. From the age of seven years, P5's infection progressed despite treatment, and he died of disseminated BCG disease at the age of eight years.

Materials and Methods

Genome-wide linkage (GWL) analysis: GWL analysis was performed as previously described (53), with minor modifications. For Kindred A, P1 was genotyped with the Affymetrix Genome-Wide Human SNP array 6.0, and six other individuals (P2, P3, II.5, II.6, III.1, III.3) were genotyped with the Affymetrix Genome-Wide Human SNP array 250K. For Kindred B, all seven individuals shown in the pedigree (Fig. 1B) were genotyped with the Affymetrix Genome-Wide Human SNP array 250K. Genotype was called with the Affymetrix Power Tools software package (http://www.affymetrix.com/estore/partners_programs/programs/developer/tools/power_tools.affx). SNPs presenting more than one Mendelian inconsistency were discarded and the remaining SNPs were filtered with population-based filters (54). For Kindred A, we used 164,052 SNP markers for linkage analysis, assuming AR inheritance with 75% penetrance, and a deleterious allele frequency of 10^{-4} . For Kindred B, we used 162,563 SNP markers for linkage analysis, assuming AR inheritance with 75% penetrance, and a deleterious allele frequency of 10^{-4} . The penetrance estimate was based on the known clinical

penetrance of IL-12R β 1 deficiency (6, 7). Parametric multipoint linkage analysis was carried out independently for each kindred with the Merlin program (55), considering the founders to be second-degree relatives. The family founders and HapMap CEU trios were used to estimate allele frequencies and to define linkage clusters, with an r^2 threshold of 0.4.

Principal component analysis (PCA): PCA was conducted using whole exome sequencing (WES) data of 3752 individuals of diverse ethnic origins from our in-house exome database and 2504 unaffected individuals of the 1000 Genomes Project as reference individuals, as described (24). The analysis was restricted to variants covered by the exome capture Agilent's SureSelect V1 with a MAF greater than 5%. The principal components were obtained using the software PLINK (54).

Whole-exome sequencing (WES): Genomic DNA was prepared from blood samples from P1, P2, P3, P4 and P5. The DNA was sheared with a Covaris S2 Ultrasonicator (Covaris), and an adapter-ligated library was prepared with the Paired-End Sample Prep kit V1 (Illumina). Exome capture was performed with the Aligent SureSelect Human Exome kit (71 Mb version), according to the manufacturer's instructions. Exome sequencing was performed by the New York Genome Center, on an Illumina HiSeq 2500 machine. The reads were aligned to the human reference genome with BWA (56), then recalibrated and annotated with GATK (57), PICARD (<http://picard.sourceforge.net/>) and ANNOVAR (58). Substitution calls were made with GATK UnifiedGenotyper, whereas indel calls were made with SomaticIndelDetectorV2. All calls with a read coverage <2x and a Phred-scaled

SNP quality of <20 were filtered out. The variants were further filtered and investigated with our in-house online server (59). All *IL12RB2* and *IL23R* mutations identified by WES were confirmed by Sanger sequencing. Familial segregation analysis was performed in both families, when the necessary material was available.

Population genetic analyses: We estimated the strength of the purifying selection acting on *IL12RB1*, *IL12RB2* and *IL23R* in humans, using an approach based on polymorphism and divergence data from synonymous and nonsynonymous sites within genes (*i.e.*, the McDonald-Kreitman table). This method, known as SnIPRE (29), uses a generalized linear mixed model to model genome-wide variability for categories of mutations and estimates two key population genetic parameters for each gene: γ , the population selection coefficient, and f , the proportion of nonsynonymous mutations that are non-lethal. We focused our investigation on the f parameter, which quantifies the strength of purifying selection acting on human genes (*i.e.*, the removal of deleterious alleles from the general population). The f parameter thus varies from 0 (all nonsynonymous mutations in the gene are lethal) to 1 (all nonsynonymous mutations in the gene are non-lethal). We first retrieved the alignment of the hg19 human genome and the PanTro3 chimp genome from UCSC Genome Browser. All differences between the two species were annotated functionally by snpEff (60), using the GRCh37.65 build. We retrieved all human CDS >20 bp long and considered, for each gene, the longest transcript available. We deduced the proportion of synonymous and non-synonymous sites in the 22,616 coding DNA sequences (CDS) obtained, accounting for gaps in human-chimp alignments. We then retrieved all polymorphisms identified in the WES data of phase 1 of the 1,000 Genomes Project (30).

We analyzed SNPs that were annotated as non-synonymous or synonymous, outside of gaps in the human-chimp alignment and polymorphic in at least one human population. We also removed from positions divergent between humans and chimps those that were actually polymorphic in humans or chimps, using the dbSNP136 chimp database. We finally obtained the number of divergent and polymorphic synonymous and nonsynonymous mutations, and the proportion of synonymous and nonsynonymous sites, in a total of 18,969 genes. SnIPRE was then used to estimate the f parameter, and genes of interest were ranked on the basis of f estimations.

Cell culture: The B-lymphoblastoid cell line (LCL-B) endogenously negative for IL-12R β 2 and IL-23R expression, positive for IL-12R β 1, STAT3, and engineered to express STAT4-iresGFP in a stable manner used, referred to hereafter as LCL-B^{STAT4}, has been described elsewhere (27). T-cell lines were generated by infecting peripheral blood mononuclear cells (PBMCs) from healthy controls or patients with *Herpesvirus saimiri*, as previously described (61). *Herpesvirus saimiri*-immortalized T (HSV-T) cells were cultured with a 1:1 mixture (by volume) of RPMI and Panserin 401 (Panbiotech), supplemented with 10% fetal bovine serum (FBS), 350 μ g/ml glutamine, 100 c/ml gentamycin, and 10 U/ml hIL-2 (Roche). Phoenix-A packaging cells (ATCC) were cultured in IMDM medium (Gibco) supplemented with 10% FCS. B-LCL^{STAT4}, Epstein-Barr virus-transformed B cells (EBV-B cells), and PBMCs were cultured in RPMI supplemented with 10% FCS. In other experiments, 300,000 HEK293T cells/well were seeded in 6-well plates. The next day, 5 μ g of pcDNA3.1-empty vector or pcDNA3.1 containing a C-terminally V5-tagged WT or Q138X *IL12RB2* were transfected in the presence of Lipofectamine reagent (Invitrogen),

per manufacturer's instructions. After 48 h, whole cell lysates (100 µg protein per lane) were subjected to SDS-PAGE electrophoresis in a 10% acrylamide/bisacrylamide gel, and the resulting bands were transferred to a PVDF membrane (Immobilon-P, Millipore). The membrane was then probed with antibodies directed against V5 (460708: Invitrogen), and GAPDH (G-9: Santa Cruz).

Production of retroviral particles: Plasmids containing the WT human *IL12RB2* (Origene #SC119132) or *IL23R* (Origene #RG211477) ORFs were obtained, and different alleles were generated by site-directed mutagenesis, with specific primers and the PFU II Hotstart PCR Master Mix (Agilent Technologies), according to the manufacturer's instructions. These ORFs were introduced into the pLZRS-IRES-ΔNGFR vector and used to generate retroviral particles, as previously described (62). Briefly, 10 µg of the retroviral vector pLZRS-IRES-ΔNGFR (empty vector), or the same vector backbone containing one of the insert sequences WT *IL12RB2*-V5, WT *IL23R*-V5, or one of the variants functionally characterized in this report, was used to transfect Phoenix-A packaging cells (ATCC) in the presence of the X-treme Gene 9 transfection reagent (Roche), according to the manufacturer's protocol. The ΔNGFR ORF encodes a truncated nerve growth factor receptor (NGFR, also known as CD271) protein that cannot transduce signal, which serves as a cell surface tag in this system. Transfected Phoenix-A cells were cultured with 2 µg/ml puromycin (Gibco) until all cells expressed ΔNGFR on their surface, as shown by flow cytometry with a PE-conjugated mouse anti-human NGFR antibody (BD Pharmingen). Phoenix-A packaging cells were cultured for another 24 h in the presence 2 µg/ml puromycin. The medium was then changed and the puromycin was removed. The virus-

containing culture supernatant was collected 24 h later. Retroviruses were concentrated from the culture supernatant with Retro-X Concentrator (Clontech), according to the manufacturer's protocol, and stored at -80°C until use.

Retroviral transduction: HVS-T cells, EBV-B cells, or LCL-B^{STAT} cells were transduced with retroviral particles by spinoculation (62). Briefly, six-well non-tissue culture treated plates were coated by incubation for 24 h with 100 ng/ml of RetroNectin (Takara) diluted in PBS. The next day, the wells were washed with PBS and the viral supernatants were thawed and added to the empty wells, and the volume in each well was made up to 2 ml with medium. Plates were centrifuged at 800 x g for 30 min and 10⁶ cells were added to each well. The plates were centrifuged for 5 min at 300 x g and incubated at 37°C for 5 days before the assessment of transduction efficiency. Transduced cells were purified by MACS, using magnetic bead-conjugated anti-NGFR antibody (Miltenyi Biotec), according to the manufacturer's protocol, and purity was confirmed, by flow cytometry, to be >95%.

Western blotting to assess the activation of STAT3 and STAT4: LCL-B^{STAT4} cells that were non-transduced, or retrovirally transduced and stably expressing the desired IL-12Rβ2 or IL-23R proteins, were left unstimulated, or were stimulated with rhIL-12 (20 ng/ml; R&D Systems), rhIL-23 (100 ng/ml; R&D Systems) or rhIFN-α2b (10⁵ units/mL, Intron-A®, Schering) for 30 min. The culture medium was removed, and the cells were washed with ice-cold PBS, and lysed in RIPA buffer (50 mM TRIS pH8, 1 mM EDTA, 150 mM NaCl, 0.5% sodium deoxycholate, 1% NP40, 0.1% SDS) supplemented with 100 mM sodium orthovanadate and Complete Mini protease inhibitor cocktail (Roche). Whole lysates (100

µg protein per lane) were subjected to SDS-PAGE electrophoresis in a 10% acrylamide/bisacrylamide gel, and the resulting bands were transferred to a PVDF membrane (Immobilon-P, Millipore). The membrane was then probed with antibodies directed against V5 (460708: Invitrogen), phospho-STAT3 Tyr705 (9145S: Cell Signaling), STAT3 (9139S: Cell Signaling), phospho-STAT4 Tyr693 (AF4319: R&D systems), STAT4 (C46B10: Cell Signaling), phospho-TYK2 Tyr1054/1055 (9321S: Cell Signaling), TYK2 (14193S: Cell Signaling), phospho-JAK2 Tyr1007/1008 (C80C3: Cell Signaling), JAK2 (D2E12 XP: Cell Signaling) and GAPDH (G-9: Santa Cruz).

Western blotting to assess IL-23R N-glycosylation: Protein lysates were prepared as described above, from LCL-B^{STAT4} cells that were non-transduced, or retrovirally transduced to express the WT or C115Y IL-23R V5-tagged proteins. Chemical inhibitors of N-glycosylation were used, as previously described (28, 63). Briefly, cells were left untreated or were treated with 166 mM kifunensine (Toronto Research Chemicals). After 48 hours, cell lysates were prepared as described above. Protein samples were then left untreated or digested overnight at 37°C with endoglycosidase-H (EndoH; Biolabs) or peptide N-glycosidase-F (PNGaseF; Biolabs) in the appropriate buffer. Immunoblotting was performed with antibodies directed against V5 (460708: Invitrogen), and GAPDH (G-9: Santa Cruz).

CXCL10 ELISA: LCL-B^{STAT4} cells that were non-transduced, or retrovirally transduced and stably expressing the desired IL-12Rβ2 or IL-23R proteins, were left unstimulated, or were stimulated with rhIL-12 (20 ng/ml; R&D Systems) or rhIL-23 (100 ng/ml; R&D

Systems) for 24 h. Cell-free supernatants were collected, and used for CXCL10 quantification by ELISA (Biolegend #439904), according to the manufacturer's protocol. Results are expressed as the fold-change difference between IL12- or IL-23-stimulated and non-stimulated cells, for each cell type.

Genetic rescue experiments: HVS-T cells were generated from the PBMCs of P1, and were left non-transduced, or transduced with retroviral particles produced with pLZRS-IRES- Δ NGFR (empty vector), or with a vector consisting of the same backbone plus WT *IL12RB2-V5*, as described above. EBV-B cells were generated from the PBMCs of P4, as described above. Cells were left non-transduced, were transduced with retroviral particles produced with pLZRS-IRES- Δ NGFR (empty vector), or with a vector containing the same backbone plus WT *IL23R-V5*, as described above.

IL12RB2 K649N mRNA splicing experiments: PBMCs were obtained from two healthy controls and a patient with a heterozygous *IL12RB2* mutation c.1947G>C, located in the first nucleotide of exon 15 and potentially causing both the K649N substitution and alternative splicing. Phytohemagglutinin (PHA)-blasts were generated by stimulating 2×10^6 PBMCs with 5 μ g/ml PHA for 72 h. Total RNA was extracted from PHA-blasts or HVS-transformed T cells with TRIzol (Invitrogen), according to the manufacturer's protocol. We generated cDNA from 5 μ g of total RNA, with the SuperScript First-Strand III Synthesis System for RT-PCR (Invitrogen). PCR was performed with primers binding between exons 12 and 15 of *IL12RB2* (5'-GCC CCG AGT GAC ATA TGT CA-3' and 5'-CTT TTT CCC TTT GTG GCC AG-3'). The PCR products were inserted into the pGEM-

T Easy vector (Promega, Madison, WI) and sequenced individually.

Ex vivo naïve and effector/memory CD4⁺ T-cell stimulation: CD4⁺ T cells were isolated as previously described (64). Briefly, cells were labeled with anti-CD4, anti-CD45RA, and anti-CCR7 antibodies, and naïve (defined as CD45RA⁺CCR7⁺CD4⁺) or effector/memory (defined as CD45RA⁻CCR7⁻CD4⁺) T cells were isolated (>98% purity) on a FACS Aria machine (BD Biosciences). Purified naïve or effector/memory CD4⁺ cells were cultured with T-cell activation and expansion (TAE) beads (anti-CD2/CD3/CD28; Miltenyi Biotec) for 5 days, and culture supernatants were then used to assess the secretion of the cytokine indicated, by ELISA (IL-22) or in a cytometric bead array (all other cytokines).

In vitro differentiation of naïve CD4⁺ T cells: Naïve CD4⁺ T cells (defined as CD45RA⁺CCR7⁺CD4⁺) were isolated (>98% purity) with a FACS Aria (BD Biosciences) machine from healthy controls or patients. They were then cultured under polarizing conditions, as previously described (64). Briefly, cells were cultured with TAE beads alone or under Th1 (IL-12 [20 ng/ml; R&D Systems]), Th2 (IL-4 [100 U/ml]; anti-IFN- γ [5 μ g/ml; eBioscience]) was also included in some cultures) or Th17 (TGF β , IL-1 β [20 ng/ml; Peprotech], IL-6 [50 ng/ml; PeproTech], IL-21 [50 ng/ml; PeproTech], IL-23 [20 ng/ml; eBioscience], anti-IL-4 [5 μ g/ml], and anti-IFN- γ [5 μ g/ml; eBioscience]) polarizing conditions. After 5 days, culture supernatants were used to assess the secretion of the cytokines indicated, by ELISA (IL-22) or with cytometric bead arrays (all other cytokines).

T-cell libraries: Two subsets of CD45RA⁻CD25⁻CD19⁻CD8⁻CD4⁺ memory T cells were sorted from total PBMC with a FACS Aria machine (BD Biosciences) on the basis of CCR6 expression. CD45RA⁺CCR7⁺ naïve cells were excluded. The CCR6⁺ subset included Th1* and Th17 cells, whereas the CCR6⁻ subset included Th1 and Th2 cells (65). The sorted memory CCR6⁻ T cells were used to seed culture plates at a density of 600 cells/well, and CCR6⁺ cells were used to seed plates at a density of 150-300 cells/well. The cells were cultured in RPMI 1640 medium supplemented with 2 mM glutamine, 1% (vol/vol) non-essential amino acids, 1% (vol/vol) sodium pyruvate, penicillin (50 U/ml), streptomycin (50 µg/ml) (all from Invitrogen) and 5% heat-inactivated human serum (Swiss Red Cross). All wells were polyclonally stimulated with 1 µg/ml PHA (Remel) in the presence of irradiated (45 Gy) allogeneic PBMCs as feeder cells (2.5×10^4 per well) and IL-2 (500 IU/ml), in a 96-well plate, and T-cell lines were expanded in the presence of IL-2, as previously described (37). After 13-16 days, a small volume of cells from three CCR6⁻ or CCR6⁺ lines from each patient were pooled and tested for their ability to produce IFN- γ , IL-17A, IL-22 or IL-4, by intracellular staining (ICS) after stimulation with PMA (200 nM) and ionomycin (1 µg/ml) (Sigma-Aldrich). The screening of the T cell lines was performed 18-22 days after initial stimulation, by culturing thoroughly washed T cells (2.5×10^5 /well) with autologous irradiated B cells (2.5×10^4), with or without a three-hour pulse with different antigens, including the *M. tuberculosis* peptide pool (0.5 µg/ml/peptide, from A. Sette's laboratory, LJI, comprising 207 peptides), the BCG peptide pool (0.5 µg/ml/peptide, from A. Sette's laboratory, LJI, comprising 211 peptides), the respiratory syncytial virus (RSV) peptide pool (1 µg/ml/peptide, from A. Sette's laboratory, LJI, comprising 190 peptides), and influenza virus (Influvac vaccine).

Proliferation was assessed on day 4, after incubation for 16 h with 1 $\mu\text{Ci/ml}$ [^3H]-thymidine (GE Healthcare). Cytokine concentrations in the culture supernatants were determined after 48 h of stimulation, in Luminex multiplex cytokine assays (Thermo Fisher). Precursor frequencies were calculated from the number of negative wells, assuming a Poisson distribution, and are expressed per million cells (66).

Purification of the leukocyte population by magnetic-activated cell sorting (MACS): Age-matched healthy donor PBMCs were stained with microbead-conjugated antibodies directed against CD20, CD56, CD8 or CD4 (Miltenyi Biotec), according to the manufacturer's protocol, or biotin-conjugated anti- $\gamma\delta\text{TCR}$ (331206: Biolegend); they were then washed in PBS, then stained with anti-biotin microbeads (Miltenyi Biotec). Labeled cells were purified by passing the cell suspension through MS columns (Miltenyi Biotec) and retaining the eluate. The purity of each cell population was shown, by flow cytometry, to be $\geq 92\%$. Leukocytes were then stimulated with rhIL-12 (20 ng/ml; R&D Systems), rhIL-23 (100 ng/ml; R&D Systems), or PMA and ionomycin (20 $\mu\text{g/ml}$ and 1 μM) for 6 h.

Leukocyte purification by FACS sorting: Healthy donor PBMCs were stained with Live/Dead fixable aqua (Invitrogen), anti-CD3 V450 (560365: BD Biosciences), anti-CD161 FITC (339923: Biolegend), anti-V α 24J α PerCPeF710 (46-5806-42: eBiosciences) and anti-V α 7.2 APC (351724: Biolegend). MAIT cells were sorted on a FACS Aria II machine (BD Biosciences) with gating on CD3 $^+$ CD161 $^+$ V α 7.2 $^+$ cells. NKT cells were sorted as CD3 $^+$ V α 24J α $^+$ cells. Sorted MAIT or NKT cells ($>95\%$ purity) were then

stimulated with rhIL-12 (20 ng/ml; R&D Systems), rhIL-23 (100 ng/ml; R&D Systems), or PMA and ionomycin (20 µg/ml and 1 µM) for 6 h.

mRNA isolation, microarray, and quantitative RT-PCR: mRNA was prepared with the ZR RNA microprep kit (Zymo Research), according to the manufacturer's protocol. mRNA samples were used to prepare biotinylated ss-cDNA fragments with the GeneChip® Whole Transcript PLUS Reagent Kit (Affymetrix), which were then hybridized to a GeneChip® Human Transcriptome 2.0 array (Affymetrix), according to the manufacturers' instructions. Data were analyzed with Affymetrix® Expression Console™ and Transcription Analysis Console software. PBMCs from three other healthy age-matched donors were stimulated as described above, mRNA was isolated and reverse transcription-PCR was performed with oligo-dT primers, according to the manufacturer's protocol (Applied Biosystems, Foster City, CA). Quantitative real-time PCR (qPCR) was performed with Applied Biosystems Taqman assays and exon-spanning probes directed against *IFNG*, *IL12RB2*, *IL12RB1* and *IL23R*, with normalization against β-glucuronidase (*GUS*), glyceraldehyde 3-phosphate dehydrogenase (*GAPDH*), or 18S housekeeping genes.

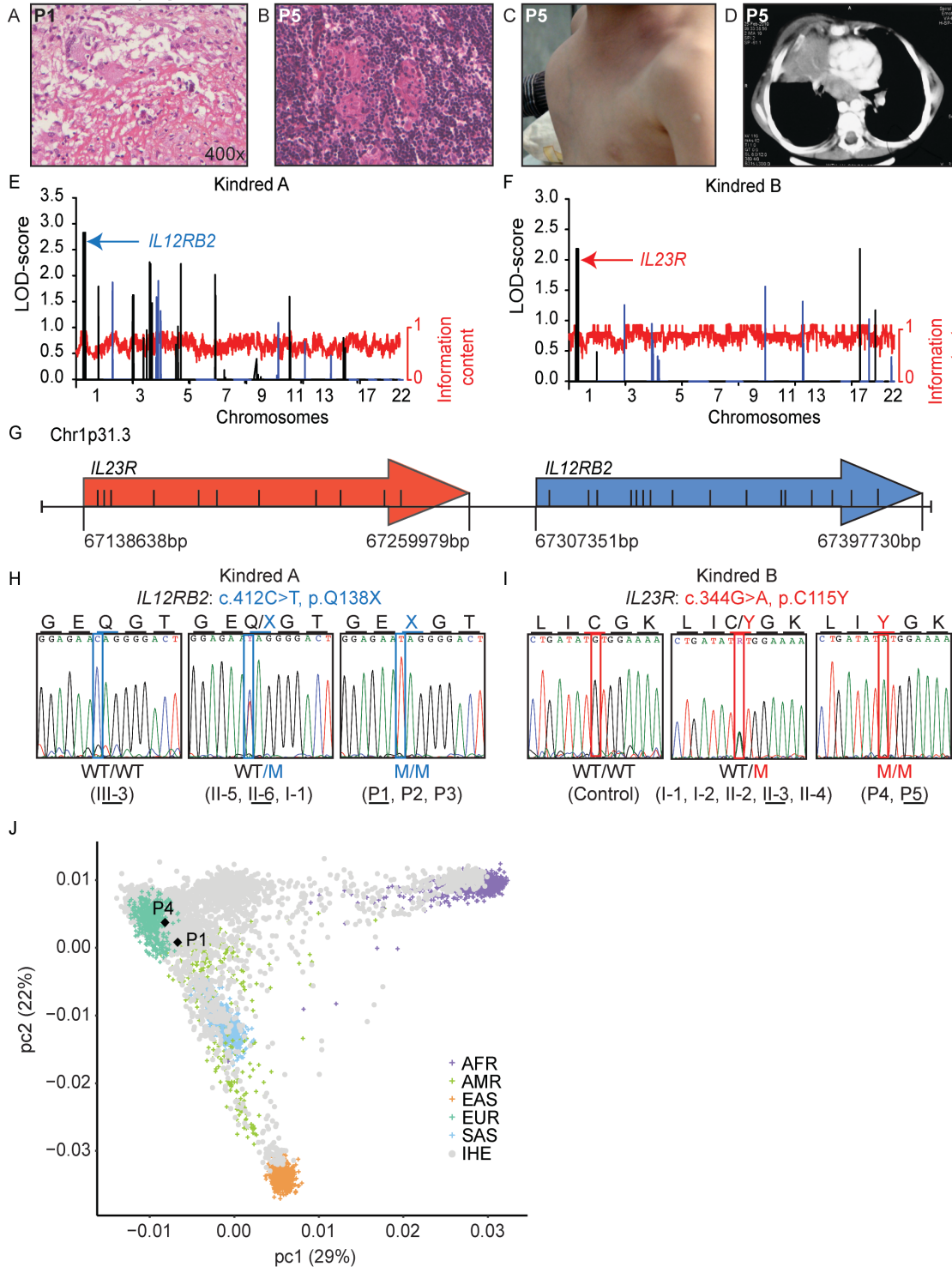
Whole-blood activation experiments: Venous blood samples from healthy controls and from patients were collected into heparin-containing tubes and processed according a modified version of the procedure described by Feinberg et al. (38). Briefly, they were diluted 1:2 in RPMI1640 (GibcoBRL) supplemented with 100 U/ml penicillin and 100 µg/ml streptomycin (GibcoBRL). We dispensed 5 ml of diluted blood sample into each of 5 wells (1 ml/well) of a 48-well plate (Nunc). These samples were incubated for 48 h at

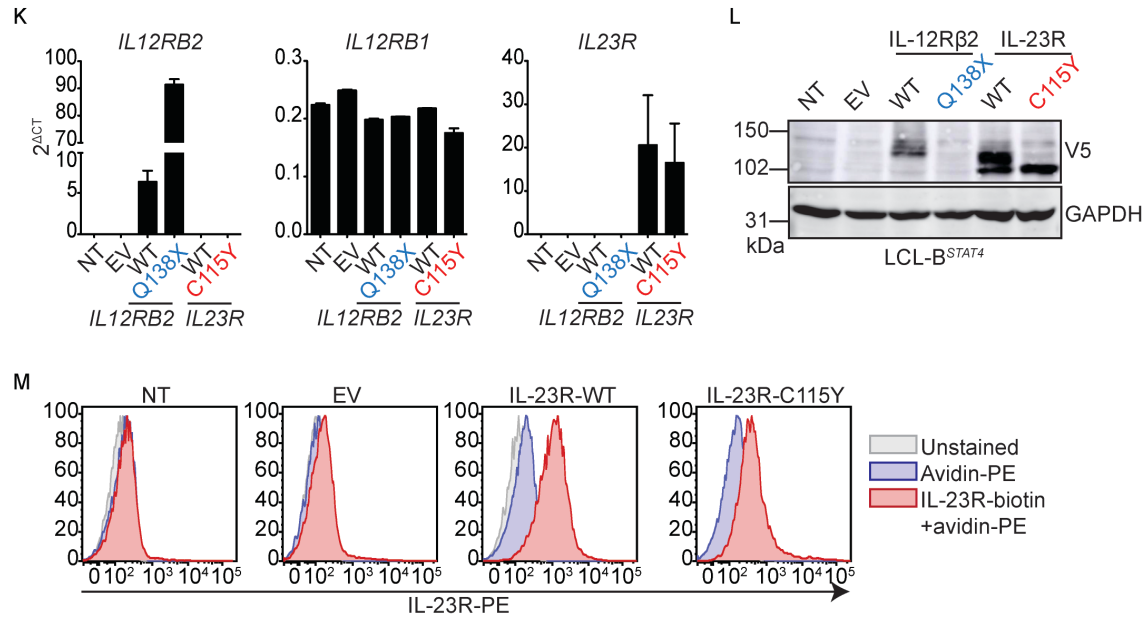
37°C, under an atmosphere containing 5% CO₂/95% air, and under three different sets of activation conditions: with medium alone, with live BCG (*M. bovis*-BCG, Pasteur substrain) at a MOI of 20 BCG bacteria/leukocyte, or with BCG plus recombinant (rh) IL-12 (20 ng/ml; R&D Systems). ELISA was performed on the collected supernatants, with the human IFN- γ ELISA Kit (Sanquin), according to the manufacturer's instructions.

PBMC activation experiments: PBMCs were isolated from buffy coats and used at a density of 10⁶/ml in RPMI medium supplemented with 10% FBS. Cells were treated with rhIL-12 (20 ng/ml; R&D Systems), rhIL-23 (100 ng/ml; R&D Systems), or live BCG (*M. bovis* BCG, Pasteur substrain) at a MOI of 20 BCG cells/leukocyte, or PMA plus ionomycin (20 μ g/ml and 1 μ M) in for 48 h. All experiments were performed in triplicate wells. Cell culture supernatants were removed and used for multiplex cytokine detection with the V-PLEX Human Proinflammatory cytokine panel assay (Meso Scale Discovery).

Supplementary figure legends

Supplementary Figure 1: Clinical and genetic features of kindreds with autosomal recessive IL-12R β 2 or IL-23R deficiency.

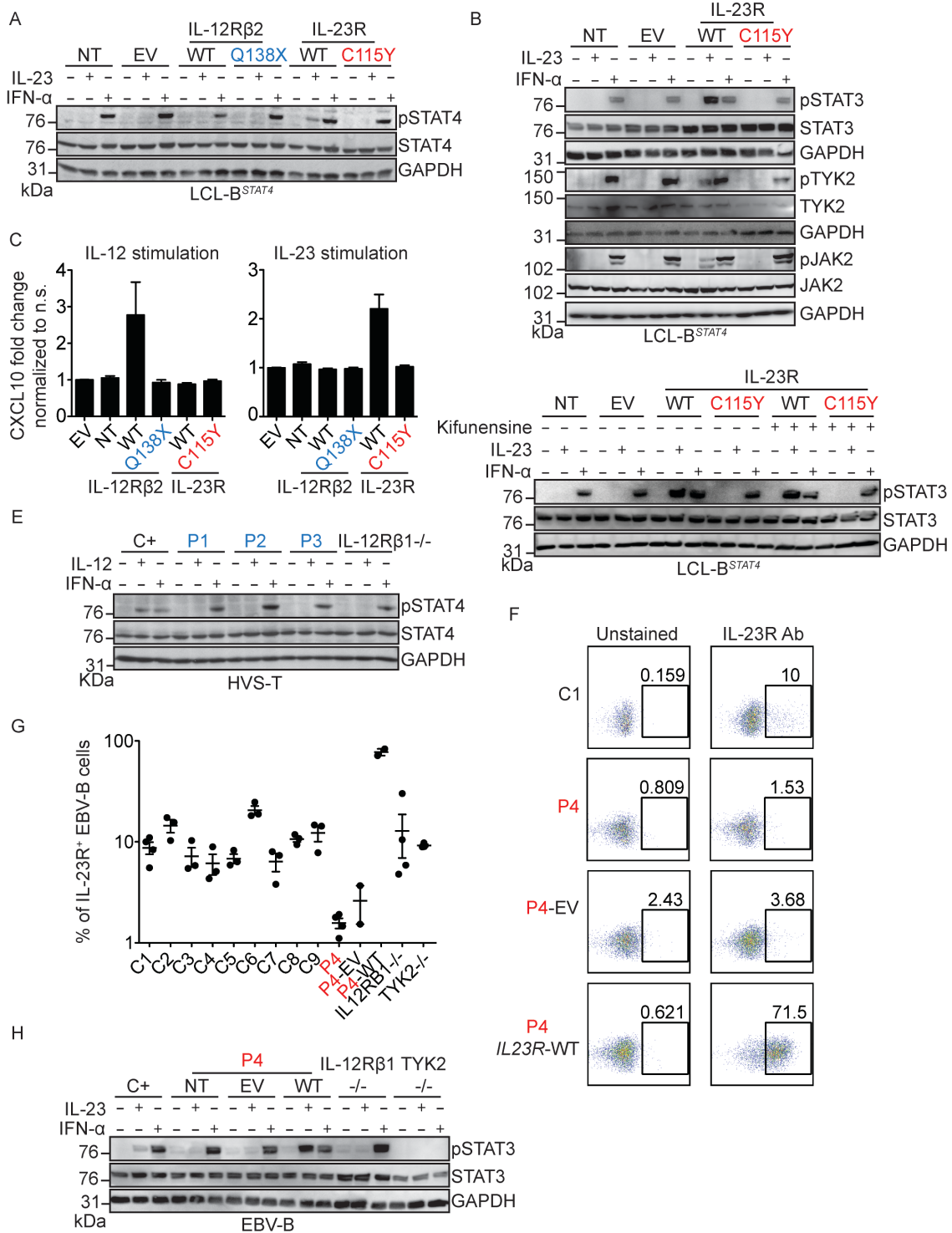


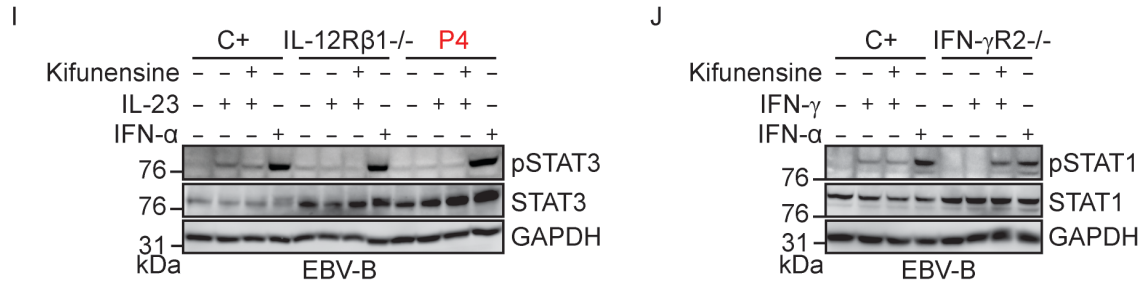


A) Histology of a lymph node biopsy specimen for P1 (*IL-12Rβ2* Q138X) showing epithelioid and multinucleated giant cells at the periphery of a necrotic area. **B)** Histology of a lymph node biopsy specimen for P5 (*IL-23R* C115Y) showing follicular hyperplasia and the presence of small ill-defined macrophagic granulomas. **C)** Gross anatomical depiction of the chest mass resulting from *Mycobacterium bovis*-BCG infection in P5 at the age of four years. **D)** CT scan of the chest, cross-sectional view, showing a mediastinal mass, in P5 at the age of four years. **E, F)** Whole-genome linkage (WGL) analysis of kindred A (E) and kindred B (F). LOD scores are shown in black and blue for alternating chromosomes, and information content is shown with a red trace. Both *IL12RB2* and *IL23R* map to the linked region of chromosome 1 indicated with an arrow. **G)** Schematic representation of the region of chromosome 1 containing *IL12RB2* and *IL23R*, located head to tail. Each arrow represents a gene, *IL23R* in red and *IL12RB2* in blue. The direction of the arrow indicates the orientation of the gene on the chromosome. The locations of the first and last nucleotide of each gene are indicated underneath the diagram. The horizontal

line represents the corresponding part of chromosome 1 and the vertical lines within each arrow indicate exon positions. **H, I**) Representative electrophoretograms corresponding to a WT individual, a heterozygous carrier and a homozygous carrier of the *IL12RB2*-Q138X (H) and *IL23R*-C115Y (I) mutations. The electrophoretograms shown are from the underlined individuals in Fig 1A-B. **J**) Principal component analysis (PCA) was performed as explained in Materials and Methods using 2,504 individuals of the 1000 Genomes Project classified in 5 populations (African (AFR), American (AMR), East Asian (EAS), European (EUR), South Asian(SAS)), and 3752 individuals of diverse ethnic origin from our in-house exome database (IHE). The two affected index cases, P1 homozygous for *IL12RB2* Q138X, and P4 homozygous for *IL23R* C115Y are shown (black diamonds). The two patients are located within clusters of individuals of our in house database who share the same origin (Turkish, and Iranian, respectively). The proportions of the variance explained by principal components (PC)1 and PC2 are shown in parentheses. **K**) LCL-B^{STAT4} cells were either left non-transduced (NT) or were transduced with a retrovirus generated with an empty vector (EV) or with a vector containing the WT or mutant V5-tagged *IL12RB2* or *IL23R*. Levels of *IL12RB2*, *IL12RB1* and *IL23R* mRNA were determined by RT-qPCR. **L**) Western blot of lysates from the same cells as in (J) with antibodies against the V5-tag, and GAPDH as the loading control. **M**) LCL-B^{STAT4} cells either non-transduced (NT) or transduced with retroviruses generated with an empty vector (EV) or with vectors containing V5-tagged WT or C115Y mutant versions of *IL23R*. Cells were then left unstained (gray trace), or were stained with an avidin-PE antibody only (blue trace), or an IL-23R-biotin antibody, washed and stained with an avidin-PE antibody (red trace). PE fluorescence is shown on the *x*-axis.

Supplementary Figure 2: *IL12RB2* Q138X and *IL23R* C115Y mutations abolish the response of the encoded receptor to its cognate cytokine ligand.

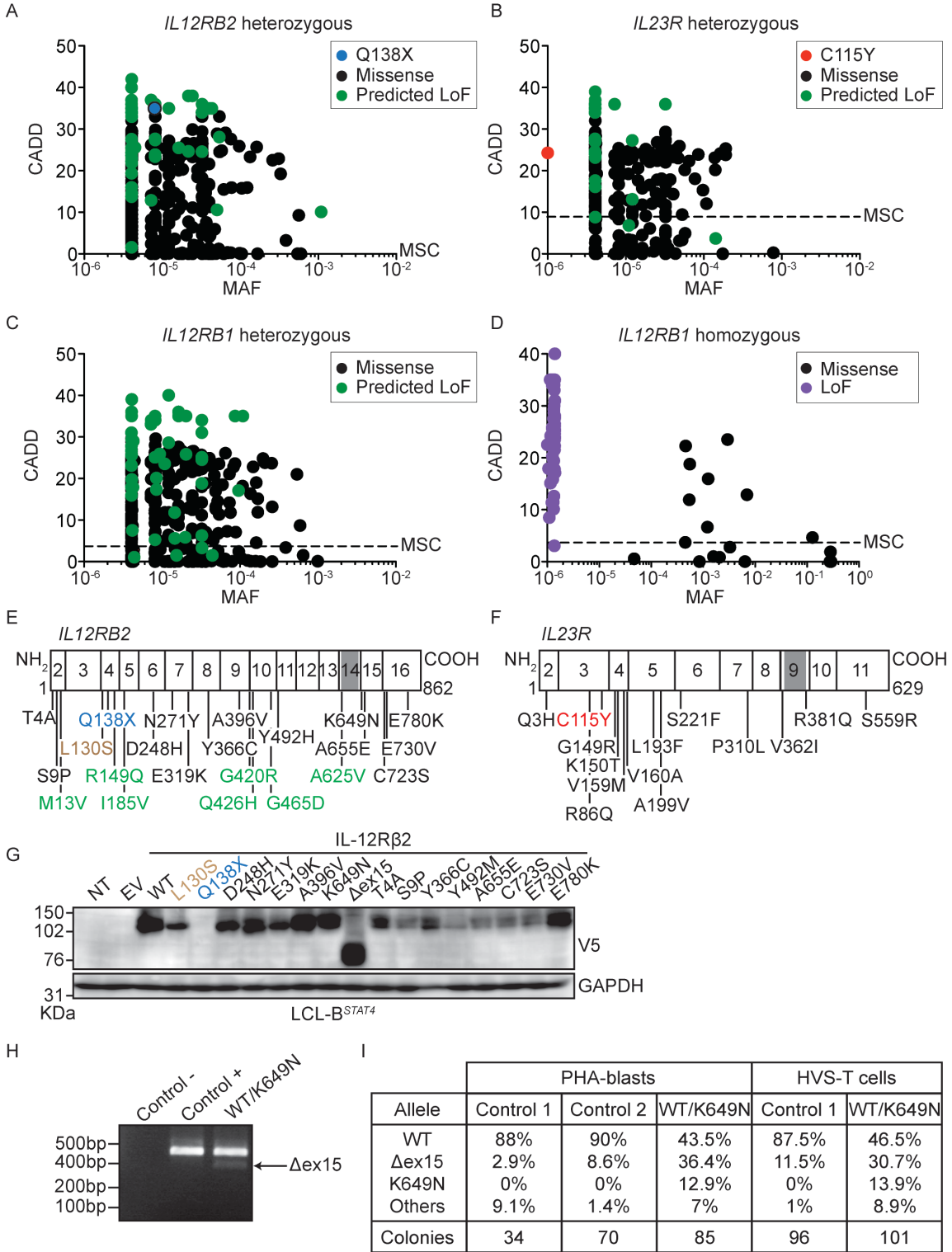


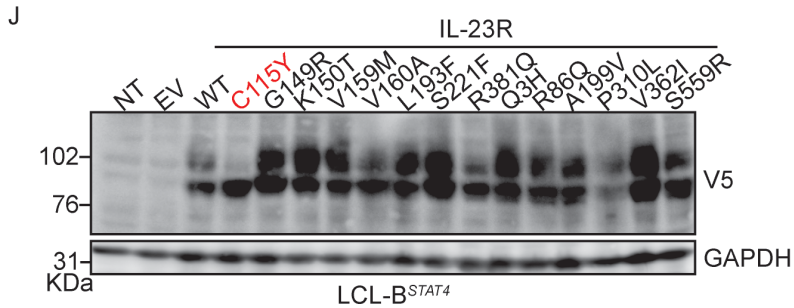


A) Western blot analysis of the same lysates as in Fig. 1I, with antibodies against phosphorylated STAT4, total STAT4 and GAPDH as a loading control. **B)** LCL-B^{STAT4} cells either non-transduced (NT) or transduced with retroviruses generated with an empty vector (EV) or vectors containing V5-tagged WT or C115Y mutant versions of *IL23R*, were either left unstimulated or were stimulated with IL-23 or IFN-α as a positive control. Lysates were analyzed by western blotting with antibodies against phosphorylated STAT3, total STAT3, phosphorylated TYK2, total TYK2, phosphorylated JAK2, total JAK2, and GAPDH as a loading control. **C)** LCL-B^{STAT4} cells were either left non-transduced (NT), or were transduced with retroviruses generated with an empty vector (EV) or vectors containing V5-tagged WT or Q138X mutant versions of *IL12RB2*, or WT or C115Y versions of *IL23R*. Cells were either left unstimulated, or stimulated with IL-12 or IL-23. After 24 h, the CXCL10 in the cell supernatant was determined by ELISA, and is expressed as a fold-change relative to unstimulated cells. **D)** The same cells as in (B) were either left unstimulated or were stimulated with IL-23 or IFN-α after 48 h of pretreatment with the glycosylation inhibitor kifunensine. Lysates were analyzed by western blotting with antibodies against pSTAT3, total STAT3 or GAPDH. **E)** HVS-T cells from a healthy control, the three IL-12Rβ2-deficient patients and an IL-12Rβ1-deficient patient were either left unstimulated or were stimulated with IL-12 or IFN-α as a positive control. They were then lysed and the lysates were subjected to western blotting with antibodies against

phosphorylated STAT4, total STAT4 and GAPDH as a loading control. **F)** FACS plots showing EBV-B cells from a representative healthy control, P4, P4 cells transduced with a retrovirus generated with an empty vector, or a vector containing WT *IL23R*, either unstained or stained for IL-23R. **G)** Percentage of EBV-B cells positive for IL-23R, for 9 healthy controls, P4, P4 cells transduced with a retrovirus generated with an empty vector (EV) or with a vector containing *IL23R-WT*, an IL-12R β - deficient patient and a TYK2-deficient patient. **H)** EBV-B cells from a healthy control (C+) P4, P4 cells transduced with a retrovirus containing *IL23R-WT*, an IL-12R β 1-deficient patient and a TYK2-deficient patient were either left unstimulated or were stimulated with IL-23 or IFN- α as a positive control. The cells were lysed and the lysates were subjected to western blotting with antibodies against phosphorylated STAT3, STAT3 or GAPDH as a loading control. **I)** EBV-B cells from a healthy control, an IL-12R β 1-deficient patient and P4 were either left unstimulated or were stimulated with IL-23 in the presence or absence of kifunensine. IFN- α stimulation was used as a positive control. Lysates were analyzed by western blotting with antibodies against phosphorylated STAT3, total STAT3 and GAPDH as a loading control. **J)** In parallel, as a control for kifunensine function, EBV-B cells from a healthy control and a patient carrying the loss-of-function *IFNGR2-382-387dup* mutation previously reported to be rescued by kifunensine treatment (28), were stimulated with IL-23 in the presence or absence of kifunensine, or with IFN- α as a positive control. The cells were lysed and the lysates were subjected to western blotting with antibodies against phosphorylated STAT1, total STAT1 and GAPDH as a loading control.

Supplementary Figure 3: Population genetics for *IL12RB1*, *IL12RB2* and *IL23R*.



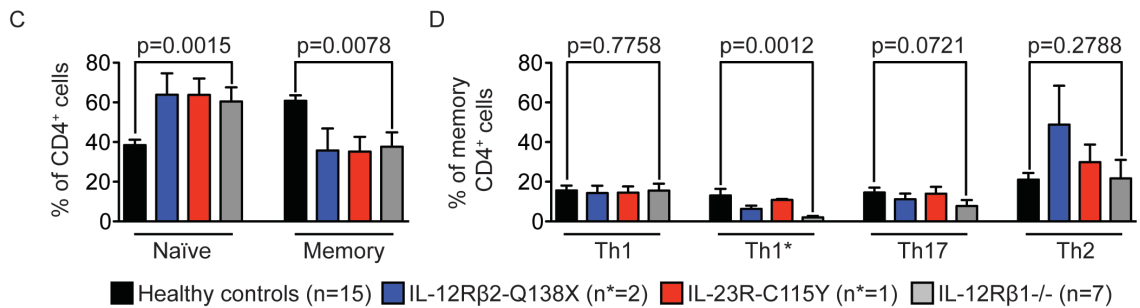
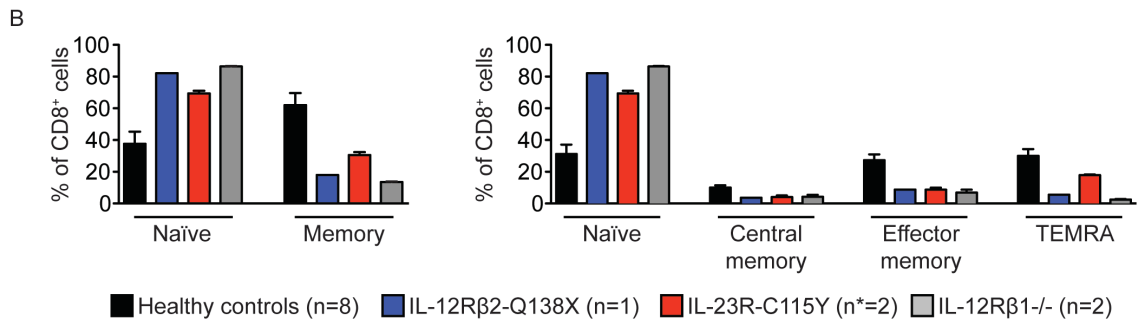
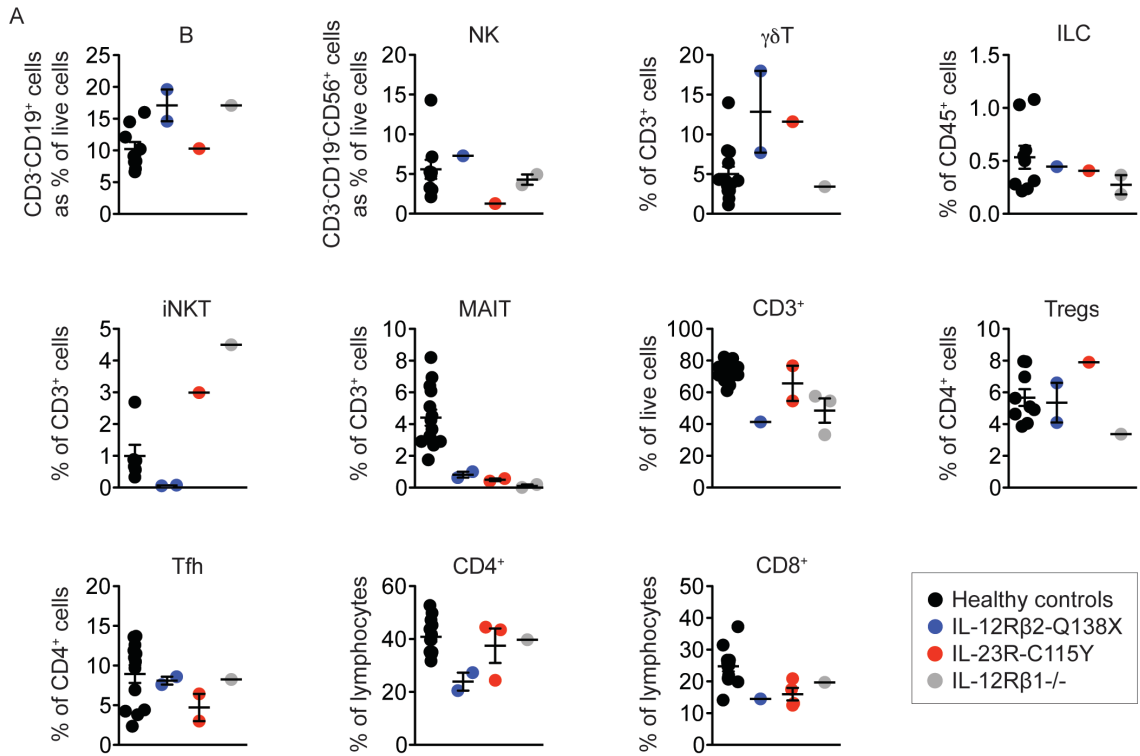


A) CADD score (y -axis) vs. minor allele frequency (MAF, x -axis) for all the heterozygous variants of *IL12RB2* found in gnomAD. The mutation studied here (Q138X) is shown in blue. Missense variants are shown in black and variants predicted to be loss-of-function (LOF; stop loss, start loss, nonsense, inframe indels, frameshift indels and essential splicing) are shown in green. **B)** CADD score (y -axis) vs. MAF (x -axis), for all the heterozygous variants of *IL23R* found in gnomAD. The mutation studied here (C115Y) is shown in red. Missense variants are shown in black and variants predicted to be LOF (stop loss, start loss, nonsense, inframe indels, frameshift indels and essential splicing) are shown in green. **C, D)** CADD score (y -axis) vs. MAF (x -axis) for all the heterozygous (C) and homozygous (D) variants of *IL12RB1* found in gnomAD. Missense variants are shown in black, and variants predicted to be LOF (stop loss, start loss, nonsense, inframe indels, frameshift indels and essential splicing) are shown in green. Variants previously demonstrated to impair or abolish IL-12R β 1 function (LoF) are shown in purple. **E)** Schematic representation of IL-12R β 2. Rectangles represent individual exons of the gene, with exon numbers indicated within the rectangles. The N-terminal portion of the protein is the extracellular domain, and gray shaded areas represent the transmembrane domain. The Q138X mutation identified in kindred A is shown in blue. *IL12RB2* variants tested by de Paus *et al.* and shown to be functional are shown in green (27). The L130S variant,

which is LOF (refer to Fig. 2E) is shown in orange and all the other variants present in the homozygous state in the gnomAD database are shown in black. **F)** Schematic representation of IL-23R. Rectangles represent individual exons of the gene with the exon numbers indicated within the rectangles. The N terminal portion of the protein is the extracellular domain, and gray shaded areas represent the transmembrane domain. The C115Y mutation identified in kindred B is shown in red. Variants present in the homozygous state in the gnomAD database are shown in black. **G)** LCL-B^{STAT4} cells were either left non-transduced (NT) or were transduced with a retrovirus generated with an empty vector (EV), a vector containing WT *IL12RB2*, or vectors containing all the homozygous *IL12RB2* variants reported in gnomAD and represented in Fig. 2C plus a plasmid containing the gene sequence but with the deletion of exon 15 described in (H, I). Lysates from these transduced cells were analyzed by western blotting with antibodies against the V5-tag and GAPDH as the loading control. **H)** cDNA was prepared from HVS-T cells from a WT donor, and from an individual heterozygous for the *IL12RB2* variant c.1947G>C. This variant may cause alternative splicing and the K649N substitution. The cDNA was amplified by PCR with primers specific to exons 14 and 16. The PCR product from HVS-T cells heterozygous for *IL12RB2* c.1947G>C gave an additional band of lower molecular weight than the WT individual, and this band corresponded to the skipping of exon 15 (Δ ex15). **I)** Using the same primers as in (H), RT-PCR was performed on PHA blasts from two WT and one heterozygous carrier of c.1947G>C, and HVS-T cells from a WT individual and a heterozygous carrier of c.1947G>C. PCR products were inserted into a pGEM-T easy vector that was then used to transform competent bacteria. Individual colonies were grown, and plasmid DNA was extracted and sequenced. This table shows

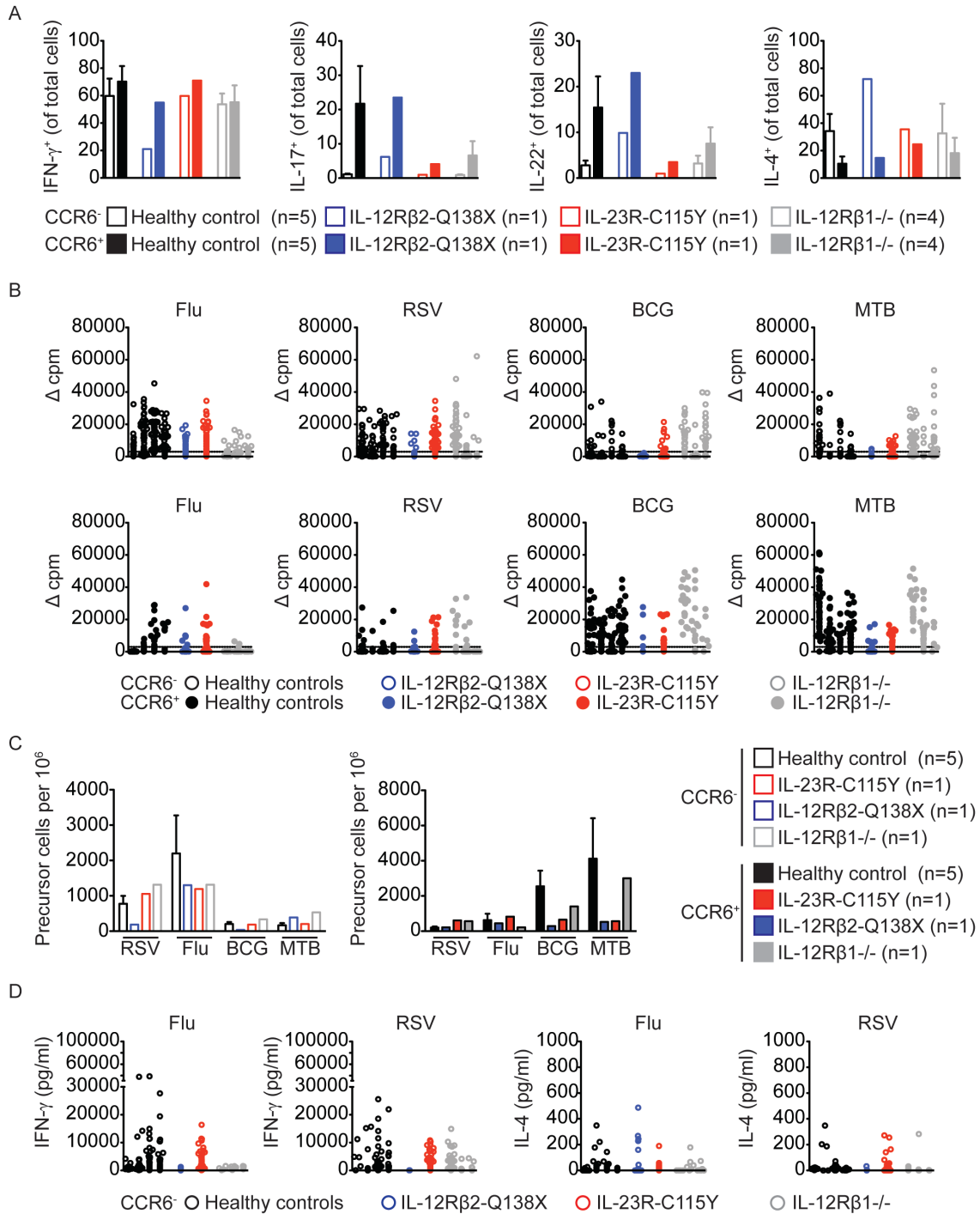
the observed *IL12RB2* genotypes corresponding to the PCR products obtained. **J)** LCL-*B^{STAT4}* cells were either left non-transduced (NT) or were transduced with a retrovirus generated with an empty vector, a vector containing WT *IL23R*, or vectors containing the homozygous *IL23R* variants reported in gnomAD and represented in Fig. 2D. Lysates from these transduced cells were analyzed by WB with antibodies against V5-tag, and GAPDH as a loading control.

Supplementary Figure 4: Immunophenotype of IL-12Rβ2-, IL-12Rβ1- and IL-23R- deficient patients.



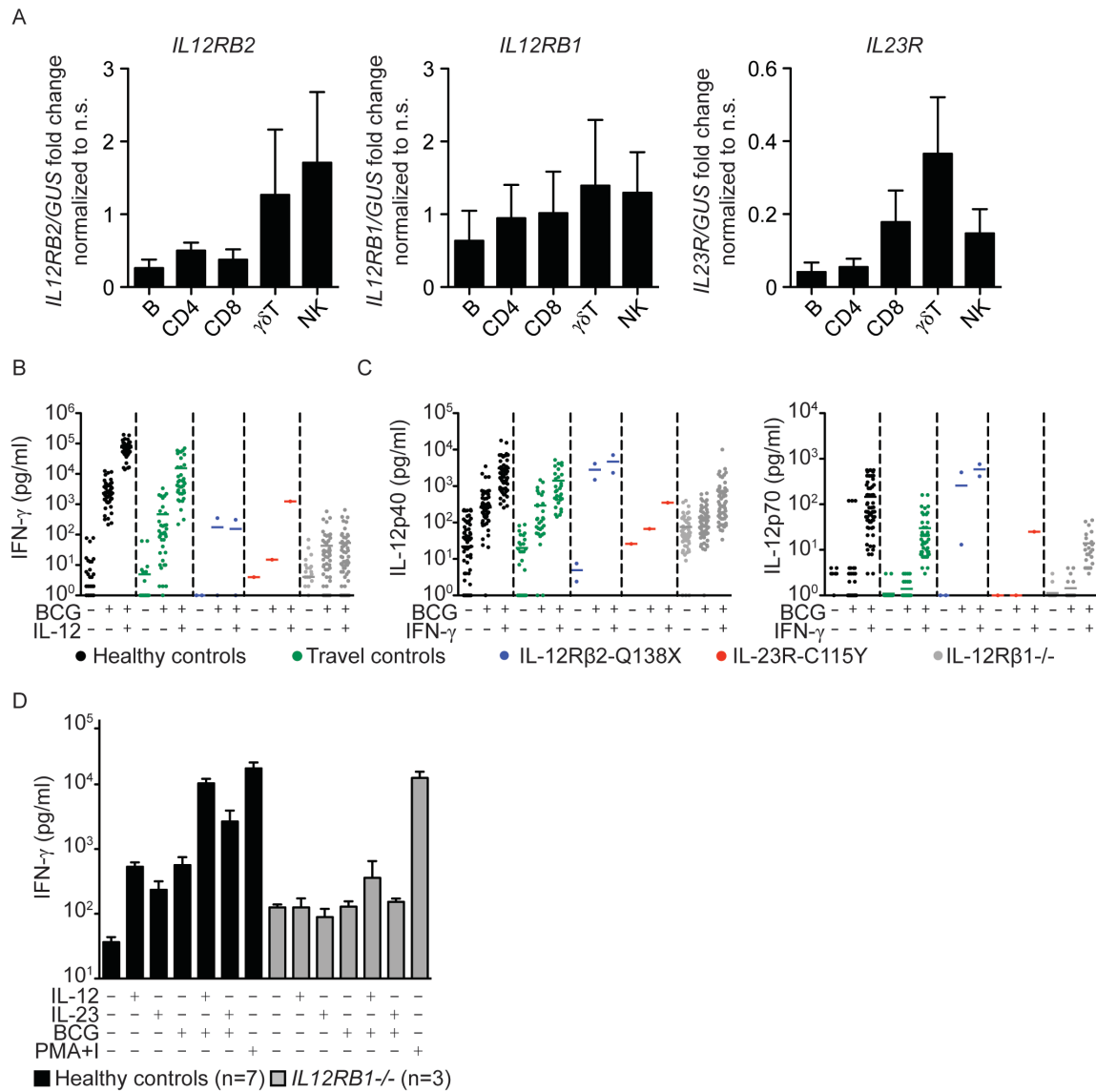
A) Frequencies of B, NK, $\gamma\delta$ T, ILC, NKT, MAIT, CD3⁺, Tregs, Tfh, CD4⁺ and CD8⁺ cells for healthy controls (black), IL-12R β 2-Q138X (blue), IL-23R-C115Y (red) and IL-12R β 1-deficient patients (gray). **B)** On the left, frequencies of naïve and memory cells, as a percentage of total CD8⁺ T cells. On the right, frequencies of naïve (CCR7⁺CD45RA⁺), central memory (CCR7⁺CD45RA⁻), effector memory (CCR7⁻CD45RA⁻) and T_{EMRA} (CCR7⁻CD45RA⁺) T cells as percentage of total CD8⁺ T cells. Error bars indicate the SEM. **C)** Frequencies of naïve and memory cells, as a percentage of total CD4⁺ T cells. **D)** Frequencies of four subsets of CD4⁺ memory T cells (CD3⁺CD45RA⁻): Th1 (CCR6⁻CCR4⁻CXCR3⁺), Th1* (CCR6⁺CCR4⁻CXCR3⁺), Th17 (CCR6⁺CCR4⁺CXCR3⁻) and Th2 (CCR6⁻CCR4⁺CXCR3⁻) were measured and expressed as a percentage of total CD4⁺ memory T cells (CD3⁺CD45RA⁻). Error bars indicate the SEM. P values for the comparison of healthy controls with *IL12RB1*^{-/-} individuals in Mann-Whitney U-tests are shown.

Supplementary Figure 5: Non-antigen-specific cytokine production, and antigen-specific proliferation, precursor frequency, and cytokine production by CD4⁺ memory T cells from healthy controls, IL-12Rβ2-, IL-23R- and IL-12Rβ1-deficient patients.



A) CCR6⁺ or CCR6⁻ memory CD4⁺ T cell lines were generated from healthy controls ($n=5$), one IL-12R β 2-Q138X patient, one IL-23R-C115Y patient, and four IL-12R β 1-deficient patients. Stimulation with PMA + ionomycin was performed on pooled T-cell lines from each patient, and the frequency of cells positive for the indicated cytokines was assessed by intracellular flow cytometry. **B)** Proliferation, measured by 3H-thymidine incorporation, of CD4⁺CCR6⁻ (upper panels) and CD4⁺CCR6⁺ (lower panels) T-cell lines stimulated by autologous B cells pulsed with influenza virus, RSV, BCG or MTB peptide pools. Healthy controls are indicated in black, IL-12R β 2-Q138X in blue, IL-23R-C115Y in red and IL-12R β 1-deficient patients in gray. **C)** Frequency (mean number per million) of RSV-, influenza virus-, BCG- and MTB-specific memory T cells within the CD4⁺CCR6⁻ (left panel) and CD4⁺CCR6⁺ (right panel) subsets in healthy controls (black), IL-12R β 2-Q138X (blue), IL-23R-C115Y (red) and IL-12R β 1-deficient patients (gray), assuming a Poisson distribution. **D)** IL-4 and IFN- γ production by influenza virus- and RSV-specific CD4⁺CCR6⁻ memory T cells.

Supplementary Figure 6: Cytokine receptor expression and responses of MAIT and NKT cells to stimulation with IL-12 or IL-23.



A) RT-qPCR for *IL12RB2*, *IL12RB1* and *IL23R* in B, CD4⁺, CD8⁺, $\gamma\delta T$, NK, NKT and MAIT cells from Fig. 4E represented as relative expression, normalized against *GUS*. **B)** Whole blood was either left non-stimulated or was stimulated with IL-12, BCG or IL-12+BCG, and IFN- γ was determined 48 h after stimulation. **C)** Whole blood was either left non-stimulated or was stimulated with IFN- γ , BCG or IFN- γ +BCG, and IL-12p40 (left)

and IL-12p70 (right) were determined 48 h after stimulation. **D)** PBMCs from healthy controls and IL-12R β 1-deficient patients were either left non-stimulated or were stimulated for 48 h with IL-12, IL-23, BCG, IL-12+BCG, IL-23+BCG or PMA+I, and IFN- γ was then determined.

Supplementary Table 1: Estimated proportions of deleterious and non-deleterious amino-acid variants in *IL12RB1*, *IL12RB2* and *IL23R*.

	<i>IL12RB1</i>	<i>IL12RB2</i>	<i>IL23R</i>
Fixed synonymous	9	11	7
Polymorphic synonymous	15	15	7
Fixed nonsynonymous	5	6	6
Polymorphic nonsynonymous	18	36	14
Synonymous sites	447.7	580	395.7
Nonsynonymous sites	1426.3	2009	1494.3
<i>f</i> estimate	46.7% [30.4% - 71.7%]	61.7% [42.1% - 90.3%]	49.0% [31.1% - 77.4%]
Genome-wide rank	50.0%	85.3%	57.0%
<i>g</i> estimate	-0.77 [-1.32 – -0.22]	-0.85 [-1.36 – -0.35]	-0.58 [-1.12 – -0.05]
Genome-wide rank	56.4%	47.9%	73.8%

Supplementary Table 2: Please refer to Auxiliary Supporting Materials and Other Supporting Files

Supplementary Table 3: Please refer to Auxiliary Supporting Materials and Other Supporting Files

Supplementary Table 4: Relative levels of IFN- γ production in response to IL-12 vs. IL-23 in different cell subsets.

Population	IL-12 (20 ng/ml)	IL-23 (100 ng/ml)
B	-	-
CD4 ⁺ T	++	+
CD8 ⁺ T	++	+
$\gamma\delta$ T	+++	++
NK	++++	+
MAIT	+	+++
NKT	+	+++
ILC1*	++	-
ILC2*	+	-
ILC3*	-	+

*Different stimulation conditions (as in Fig 4A)